Am. J. Trop. Med. Hyg., 86(2), 2012, pp. 320–327
doi:10.4269/ajtmh.2012.11-0395

Human Risk of Infection with *Borrelia burgdorferi*, the Lyme Disease Agent, in Eastern United States

Maria A. Diuk-Wasser,* Anne Gatewood Hoen, Paul Cislo, Robert Brinkerhoff, Sarah A. Hamer, Michelle Rowland, Roberto Cortinas, Gwenaël Vourc'h, Forrest Melton, Graham J. Hickling, Jean I. Tsao, Jonas Bunikis, Alan G. Barbour, Uriel Kitron, Joseph Piesman, and Durland Fish

Yale School of Public Health, New Haven, Connecticut; Michigan State University, East Lansing, Michigan; Institut National de la Recherche Agronomique, Saint Genès Champanelle, France; California State University, Monterey Bay, Seaside, California; University of California, Irvine, California; Centers for Disease Control and Prevention, Fort Collins, Colorado; Dartmouth Medical School, Lebanon, New Hampshire; University of Richmond, Richmond, Virginia; Magee-Women's Hospital of UPMC, Pittsburgh, Pennsylvania; University of Nebraska, Lincoln, Nebraska; University of Tennessee, Knoxville, Tennessee; Vilnius University, Vilnius, Lithuania; Emory University, Atlanta, Georgia

Abstract. The geographic pattern of human risk for infection with *Borrelia burgdorferi* sensu stricto, the tick-borne pathogen that causes Lyme disease, was mapped for the eastern United States. The map is based on standardized field sampling in 304 sites of the density of *Ixodes scapularis* host-seeking nymphs infected with *B. burgdorferi*, which is closely associated with human infection risk. Risk factors for the presence and density of infected nymphs were used to model a continuous 8 km × 8 km resolution predictive surface of human risk, including confidence intervals for each pixel. Discontinuous Lyme disease risk foci were identified in the Northeast and upper Midwest, with a transitional zone including sites with uninfected *I. scapularis* populations. Given frequent under- and over-diagnoses of Lyme disease, this map could act as a tool to guide surveillance, control, and prevention efforts and act as a baseline for studies tracking the spread of infection.

INTRODUCTION

Lyme disease, the most prevalent vector-borne disease in the United States is caused by *Borrelia burgdorferi* sensu stricto, a tick-borne spirochete. In the eastern United States, the bacterium is maintained in a horizontal transmission cycle between its vector, the black legged tick *Ixodes scapularis,* and vertebrate reservoir host species. Humans are incidental hosts, acquiring the pathogen through tick bites. Most patients develop a distinctive rash, erythema migrans, which is accompanied by flu-like symptoms such as fatigue, headache, mild stiff neck, joint and muscle aches, and fever.[1] In some untreated cases, symptoms of disseminated disease involving neurologic, cardiac, or articular complications, may develop weeks or months after exposure.[2] Since initially described in Lyme, Connecticut,[3] the disease has steadily increased in incidence and expanded its geographic range,[4] causing a regional epidemic in the eastern United States and southeastern Canada.

Accurate information on spatial patterns of human risk of exposure to infected ticks is essential for the public to make personal protection decisions and for efficient allocation of public health resources. Delineation of Lyme disease-endemic areas also assists local medical communities in considering a diagnosis of tick-borne disease. Accurate and timely diagnosis is critical as delay may lead to severe disease requiring more aggressive treatment.[5] On the other hand, overuse of antibiotics sometimes results in serious negative outcomes, potentially including death.[6,7] Considering the 2.7 million diagnostic assays for *B. burgdorferi* that are conducted annually in the United States,[8] even a small proportion of false positive results could dwarf the number of reported cases (~20,000 cases/year[4]) and result in a skewed distribution of case reports. Finally, accurate information on local exposure risk can guide the use of antimicrobial prophylaxis for the prevention of Lyme disease after a recognized tick bite, currently recommended where tick infection prevalence is greater than 20%.[9]

The Lyme disease case definition currently adopted by the Centers for Disease Control and Prevention (CDC) considers endemic those counties with at least two confirmed, locally acquired cases or in which established populations of a known tick vector are infected with *B. burgdorferi*.[10] However, significant Lyme disease underreporting and misdiagnosis[4] and geographic expansion in vector distribution limit the reliability of using past human cases to predict risk. In addition, the variable interval between time of exposure to infected ticks and manifestation of symptoms confounds the precise determination of exposure location, and can result in the incorrect association of cases with specific counties. Acarological risk, as measured by the density of infected host-seeking *I. scapularis* nymphs has been previously found to be positively correlated to Lyme disease incidence on a regional scale[11] and is free of some of the biases involved in human case reporting.

The use of geographic information systems and remote sensing techniques to map vector-borne diseases has evolved significantly over the past 25 years. The convergence of factors such as the availability of multi-temporal satellite data and sophisticated statistical and image processing algorithms have provided the necessary tools to generate predictive surfaces of disease risk based on vector or human case data that can be used to guide prevention and interventions (reviewed in Reference 12).

We developed an acarological risk map for Lyme disease based on standardized field sampling to estimate the density of *B. burgdorferi*-infected host-seeking nymphal *I. scapularis* throughout the range of the tick. We focused on the nymphal stage because it is the only tick life stage that has a significant role as a vector for *B. burgdorferi* in eastern North America[11,13] as a result of its small size, propensity to feed to repletion on humans, and summer host-seeking activity. Building on our previous research to identify the environmental predictors for the density of ticks,[14] here we assess environmental predictors for nymphal infection prevalence and combine them to model

*Address correspondence to Maria A. Diuk-Wasser, 60 College St., P.O. Box 208034, New Haven, CT 06520-8034. E-mail: maria.diuk@yale.edu

a continuous predictive surface of human risk of exposure to infected ticks independent of human case reports.

METHODS

Tick sampling scheme. The study area included the continental United States east of the 100th meridian (37 states), encompassing the known *I. scapularis* distribution.[15] A spatially stratified random design was applied by overlaying a two-degree sampling grid across the study area; state parks or other publicly accessible forested areas were randomly selected within each grid cell. A total of 304 sites were sampled between 2004 and 2007, 30 of which were repeatedly sampled in 2 to 4 years, resulting in a total of 348 site-year samples. No infection data were available for four sites resulting in 344 site-years. Within each site, we measured relative nymphal density by drag sampling[16] of closed-canopy deciduous forest along five 200 m transects. To capture the host-seeking phenology of *I. scapularis* nymphs, we visited sites a median of five times during late spring and summer (range: 1–6), when nymphs actively seek their hosts in the northeastern United States.[17] Sampling was performed between 19 May and 27 August in 2004, 9 May and 4 October in 2005, 10 May and 30 September in 2006, and 8 May and 4 August 2007. In 2007, data on tick density was not collected; therefore, only infection prevalence data are reported. Additional details of the sampling methodology are described in a previous publication with focus on modeling the distribution of host-seeking nymphs.[14]

Tick processing and calculation of the density of infected *I. scapularis* nymphs (DIN). The dependent variable in the analysis to follow is the annual mean density of infected nymphs per 1,000 m^2. This was derived from multiplying the density of nymphs per 1,000 m^2 by the infection prevalence at each site-year. The estimated annual mean density of nymphs per 1,000 m^2 was derived by 1) calculating the mean number of *I. scapularis* nymphs collected per visit by averaging the collections from the five transects; 2) representing the observed phenology at a site by plotting the mean number of nymphs per visit by time; 3) calculating the area under phenology curve; and 4) dividing this area by the total number of days elapsed between the first and last sampling visit at a site for a given year.[14]

Following ammonium hydroxide total DNA extraction, the presence of *B. burgdorferi* DNA was determined for all *I. scapularis* nymphs in 344 of the sites/years by polymerase chain reaction amplification of a portion of the 16S rRNA gene with species-specific primers.[18]

Infection prevalence was calculated for each collection site-year by dividing the total number of *B. burgdorferi*-positive nymphs by the total number tested at each site-year. The prevalence estimate at each site was used to calculate the density of infected nymphs, regardless of sample size. We assumed infection prevalence did not vary over one transmission season.

Environmental covariates. The environmental covariates evaluated as predictors of the density of infected nymphs were selected from among those found to be associated with the density of host-seeking *I. scapularis* nymphs,[14] in addition to landscape metrics describing forest fragmentation patterns that we hypothesized to be indirectly associated with nymphal infection prevalence with *B. burgdorferi*. Smaller forest fragments have been linked to higher abundance and infection prevalence of nymphal *I. scapularis*.[19,20]

Factors potentially influencing I. scapularis nymphal density. Our previous model of nymphal density[14] assessed a large number of variables (Supplementary Technical Appendix). On the basis of the best predictive model for the density of nymphs, we included in the current model elevation, mean vapor pressure deficit (VPDm), the annual amplitude of the maximum temperature cycle (TMAXaa), the annual phase of the minimum temperature cycle (TMINap), the annual amplitude of the normalized difference vegetation index (squared, NDVIaa), and an autocovariate term that accounts for the expectation of sites closer in space to be more similar to one another than sites farther apart.[14]

Factors potentially influencing B. burgdorferi nymphal infection. We used data derived from the 30 m resolution 2001 National Land Cover Database (NLCD[21]) to characterize spatial patterns in the distribution of deciduous and mixed deciduous-evergreen forest cover and fragmentation in 8 km × 8 km cells centered on each of our sampling sites. Each cell included 71,111 30 m NLCD pixels, and we calculated the following fragmentation metrics using Fragstats (version 3.3, Amherst, MA): total area, proportion of the landscape occupied by deciduous-mixed forest, number of deciduous-mixed forest patches, total linear edge between deciduous-mixed forest and other land cover types, proportion of the landscape occupied by the largest deciduous-mixed forest patch, mean deciduous-mixed forest patch area, average Euclidean distance between nearest-neighbor deciduous-mixed forest patches, an index of total aggregation of deciduous-mixed forest patches, an index of mean edge/area ratio for deciduous-mixed forest classes, and perimeter-area fractal dimension. We also calculated Shannon's and Simpson's diversity indices using all classes included in the 2001 NLCD ($N = 27$) independently, but collapsing deciduous and mixed forest.

After preprocessing the data, the values of the environmental data sets corresponding to each site were extracted for the point location of each site from the closest 8 km × 8 km pixel.

Model development. We developed a zero-inflated negative binomial (ZINB) regression model for the expected density of infected *I. scapularis* nymphs using environmental covariates as predictors (countreg procedures, SAS software, SAS Institute Inc., Cary, NC). The ZINB regression model is used for data that appears to have a negative binomial distribution with an excess number of zero-valued observations. The ZINB regression model simultaneously uses a logistic function to model the process that is generating the excess zeros and a negative binomial regression function to model the process that is generating the remaining data.[22]

We used a modified forward stepwise procedure to select the variables to include in the model. We initially included all variables present in the model for the density of host-seeking nymphs[14] and subsequently added a single variable to either the logistic or the negative binomial components of the model. At each step, we identified the best fit model as the one where all variables were significant ($P < 0.05$) and had the lowest Akaike information criterion. Variables were added until there were no improvements in the model fit.

Risk map generation. The acarological risk map was developed by running the selected regression model using the values of the environmental predictors at each pixel location. In addition to presenting a continuous surface of acarological risk, we generated confidence bands for the predicted surface. A confidence band (CB) essentially estimates the 95% confidence

interval (CI) for the entire range of expected values produced by the regression function. In contrast with simple regression models, for which a closed form solution can be calculated for the joint distribution of regression parameters, such closed form solution is not readily available for the ZINB. Therefore, we used bootstrap simulations to generate CIs for each density estimate produced in our analysis. Collectively, these bootstrap CIs form an estimate of the confidence band or confidence surface for the regression function. To generate these CIs, a total of 10,000 pseudo-samples of size 344 were created by randomly selecting (with replacement) from the data set used to do the original analysis. The ZINB regression model used for the original analysis was applied to each pseudo-sample, resulting in estimates of density of infected nymphs for every pixel. By ranking the estimates for a pixel and identifying the 5th and 95th percentiles, an empirical estimate for the upper and lower bootstrap confidence surface was obtained for the original estimates of our regression model. High-risk areas were defined as those for which the lower bound of the 95% CB was larger than a threshold number of infected nymphs and low risk were those for which the upper bound of the 95% CB was smaller than the threshold number of infected nymphs. Transitional areas were defined as those neither in the high nor low risk categories. A range of thresholds were examined and the one that maximized the sensitivity of the model was selected for the final risk map (Supplementary Figure S1).

RESULTS

Density of *I. scapularis* nymphs per 1,000 m^2. A total of 5,332 *I. scapularis* nymphs were collected at 94 sites (107 site-years) out of 304 sites (344 site-years) (30.1%) sampled between 2004 and 2006, with yearly totals in positive sites ranging from 1 to 506. The weighted mean density of host-seeking nymphs per 1,000 m^2 was 3.28 (s.d. 10.53), ranging from 0 to 101.29 (Supplementary Table 1). Two population foci were identified in the Northeast and upper Midwest, with no nymphs collected between these two regions (in and around Ohio). A map and details of the nymphal density data have been previously published.[14]

The DIN per 1,000 m^2 was derived for each site-year by multiplying the annual mean density of host-seeking *I. scapularis* nymphs (DON) by the infection prevalence at each site-year. Mean DIN was 0.64 (s.d. 2.24), ranging from 0 to 18.62 (Figure 1). Two discontinuous acarological risk foci were identified, one from northern Virginia to southern Maine and one in the upper Midwest, centered in Wisconsin and Minnesota. The density of infected nymphs per 1,000 m^2 was not significantly different between the two foci or between sites with high and low density of nymphs, split at the median (Mann-Whitney two-sample statistic, $P < 0.05$).

The ZINB model for the density of infected host-seeking *I. scapularis* nymphs with the lowest Akaike information criterion and for which all covariates were significant ($P < 0.05$) included elevation, VPDm, and TMINaa as predictors for the absence of infected nymphs. The spatial autocovariate term and the proportion of the landscape occupied by the largest deciduous-mixed forest patch were significant positive predictors for the density of infected nymphs in positive sites (Table 1). No spatial autocorrelation was detected in the residuals of the regression model (Moran's I $Z = -1.28$, $P = 0.19$).

TABLE 1

Zero-inflated negative binomial model of the density of infected host-seeking *Ixodes scapularis* nymphs

	Estimate	Std error	*t* value	Pr > |*t*|
Zero Inflated				
Intercept	1.20	0.70	1.83	0.07
Elevation	4.07	1.06	3.38	< 0.001
Vapor pressure deficit mean	5.32	1.43	3.72	< 0.001
TMIN annual phase	2.24	0.66	3.41	< 0.001
Negative Binomial				
Intercept	−0.82	0.44	−7.86	0.06
Autocovariate term	0.64	0.16	4.04	< 0.0001
Largest forest patch index	0.62	0.22	2.82	< 0.001

TMIN = monthly minimum temperature.

A threshold of 0.3 infected nymphs per 1,000 m^2 was selected to define high- and low-risk areas; the model's sensitivity was maximized using this threshold, although retaining a high model specificity and overall accuracy (Supplementary Figure S1). Of the 344 site-years sampled, 279 were classified with 95% confidence using this threshold, 62 as high risk and 217 as low risk (Figure 2), with just three high-risk sites misclassified as low risk. Accuracy and precision metrics are presented in Table 2.

***Borrelia burgdorferi* nymphal infection prevalence.** *Ixodes scapularis* nymphs from 92 of the sites (5,328 nymphs; 4 nymphs from 2 sites could not be processed) were tested for the presence of *B. burgdorferi* DNA. Overall infection prevalence was 0.20 (1,044 positive nymphs/5,328 nymphs tested). At least one positive nymph was collected in 50 sites (61 site-years). Of the remaining 42 sites, in only 4 sites we sampled > 14 nymphs, which we estimated as the threshold to be 95% confident that the site is negative based on the binomial probability distribution. Two of these sites were located along the Illinois-Indiana border and two along the New York-Vermont border (Figure 3).

We selected a subsample of sites with a minimum of 100 nymphs per sampling year to examine spatial and temporal patterns in infection prevalence (Figure 4). We used a binomial log-likelihood probability function to estimate 95% CIs for each prevalence estimate.

DISCUSSION

Climate and landscape-based modeling of Lyme disease acarological risk revealed two discontinuous population foci

TABLE 2

Accuracy and precision of the binary risk classification of the sites identified as high and low risk, excluding the sites classified as being in the transition zone*

		Observed		
		High risk	Low risk	
Predicted	High risk	39	23	62
	Low risk	3	214	217
		42	237	279
Accuracy			0.91	
Sensitivity			0.93	
Specificity			0.90	
Positive predictive value (precision)			0.63	
Negative predictive value			0.99	

*Observed high-risk sites were those in which at least 0.3 infected nymphs per 1,000 m^2 were collected; observed low-risk sites were those in which < 0.3 infected nymphs per 1,000 m^2 were collected; predicted high-risk sites were those in which the lower limit of the bootstrap 95% confidence interval (CI) was higher than 0.3; predicted low risk sites were those in which the upper limit of the 95% bootstrap CI was < 0.3.

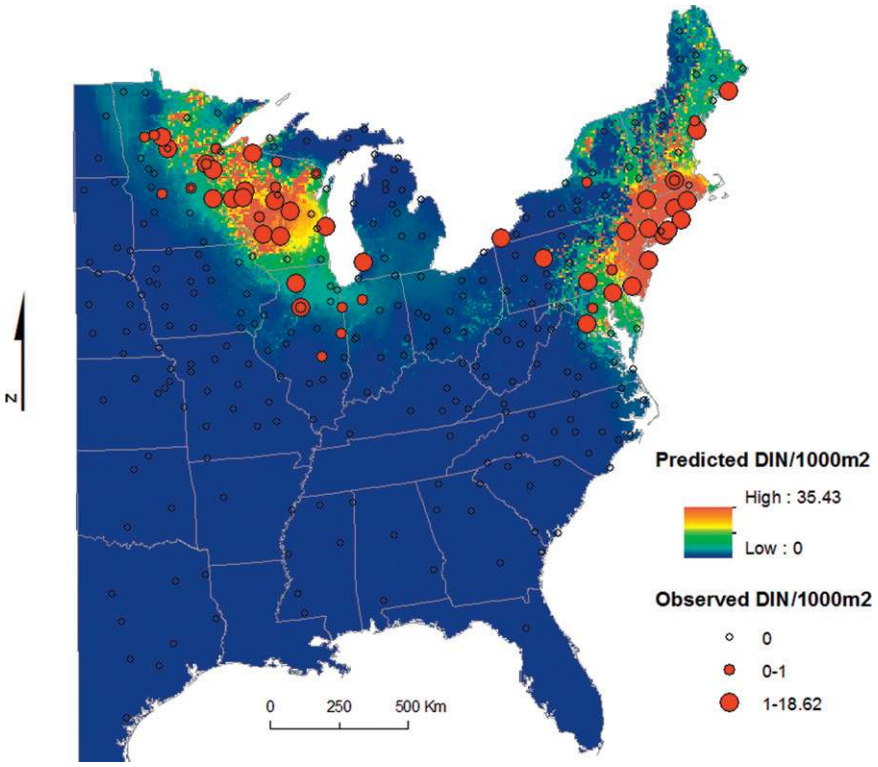

FIGURE 1. Predicted and observed density of infected host-seeking *Ixodes scapularis* nymphs (DIN)/1,000 m^2.

for both *B. burgdorferi* and *I. scapularis*, one in the Northeast and one in the upper Midwest. The ZINB modeling approach allowed for the identification of separate sets of variables for predicting presence/absence and density of infected nymphs. Lower elevation, low vapor pressure deficit, and low seasonal extremes in minimum temperature were associated with the presence of infected nymphs. No nymphs were collected above a threshold elevation of 510 m. The less fragmented

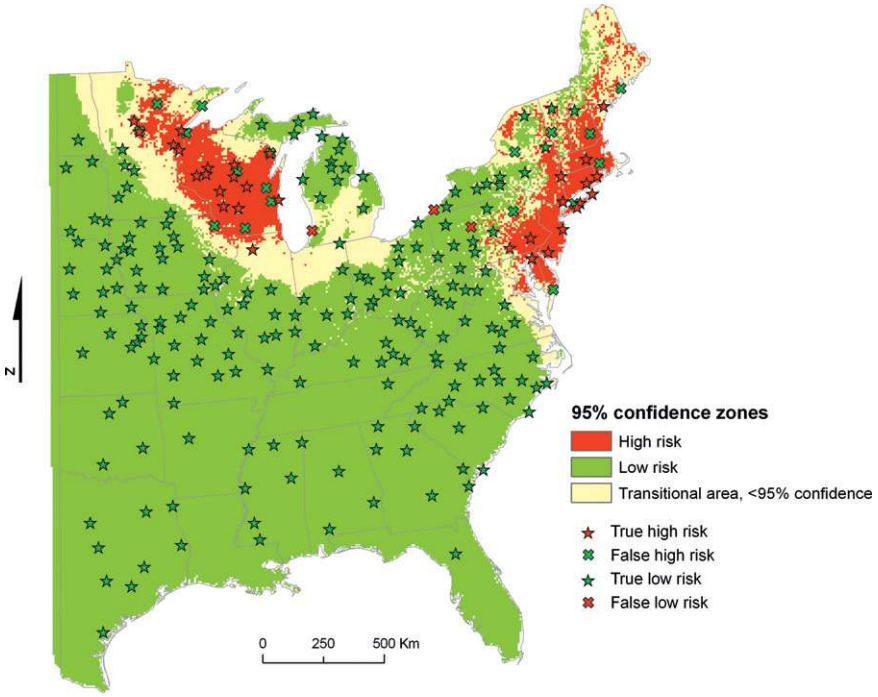

FIGURE 2. Statistically significant high- and low-risk areas. High risk: 95% probability that at least 0.3 infected nymphs will be collected per 1,000 m^2; low risk: 95% probability that < 0.3 infected nymphs will be collected per 1,000 m^2; transitional area: risk cannot be ascertained with 95% confidence (confidence interval includes 0.3); true high risk: > 0.3 infected nymphs collected in a predicted high-risk area; true low risk: < 0.3 infected nymphs collected in a predicted low-risk area; false high risk: < 0.3 infected nymphs collected in a predicted high-risk area; false low risk: > 0.3 infected nymphs collected in a predicted low-risk area.

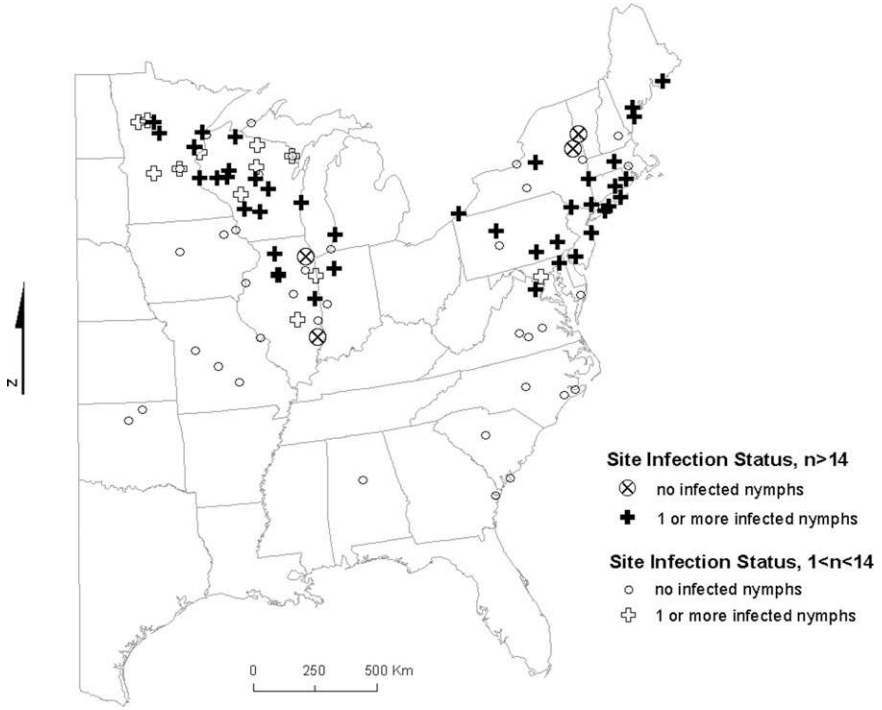

FIGURE 3. Infection status of sites where at least one *I. scapularis* nymph was collected. Sites where at least 14 nymphs were collected between 2004 and 2006 are highlighted. With this sample size and assuming infection prevalence of 0.20, it is estimated with 95% confidence that at least one infected nymph would have been collected were the site positive.

landscapes were associated with higher densities of infected nymphs in positive sites. The density of infected nymphs was also associated with the density of infected nymphs in nearby sites, as represented by the autocovariate term. The spatial dependency captured by this term is likely caused by recent and ongoing population expansion of *I. scapularis* from past refuges in the Northeast[23] and the upper Midwest[24] following environmental changes such as reforestation, suburbanization, and reintroduction of deer.[25] The inclusion of an autocovariate term captures an important feature of this ongoing expansion, that is, the so far unrealized occupation of all suitable habitats by *I. scapularis*, a consequence of constraints on dispersal or establishment.[26]

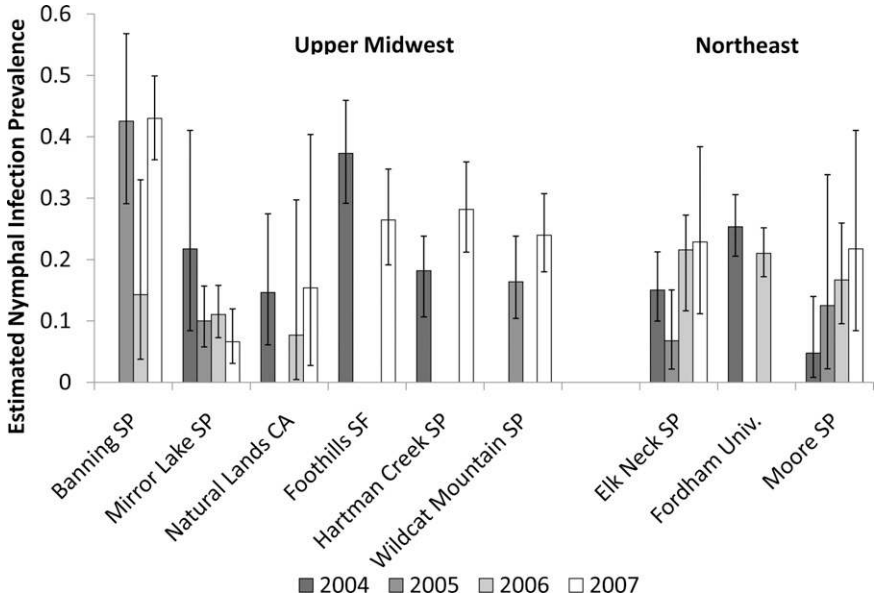

FIGURE 4. *Borrelia burgdorferi* prevalence estimates in nymphal *I scapularis* for sites repeatedly sampled with a minimum of 100 nymphs collected in each of the sampled years. We used a binomial log-likelihood probability function to estimate 95% confidence intervals for each prevalence estimate.

The absence of host-seeking nymphs infected with *B. burgdorferi* in the southern portion of the range of *I. scapularis* is consistent with previous studies.[27,28] Although *I. scapularis* populations are present in this region, the nymphs have an altered feeding behavior presumably adapted to lizards and skinks and cannot be readily sampled by the drag cloth collecting method.[14] Because this method is directly correlated with human contact with host-seeking ticks, it is considered a direct measure of risk for tick bites.[11,29] The absence of infected host-seeking nymphal *I. scapularis* in most southern states suggests that reported cases from this region may be mostly caused by either misdiagnosis or travel to an endemic area.

The threshold for classifying areas into low and high risk was selected to maximize the sensitivity of the model, given the high potential cost of underestimating risk of infection. Using this threshold, the final model had 91% accuracy, 93% sensitivity, and 90% specificity. The model predicted the presence of infected nymphs in some negative sites for which other sources indicate emerging risk, such as eastern Maine,[30] the Illinois/Indiana border,[24,31] the New York/Vermont border,[32] southwestern Michigan,[33] and eastern North Dakota (Vaughan J, personal communication). The density of infected nymphs was often underestimated by the model in these regions, and bootstrap CIs often included the threshold value for infected nymphs, therefore the sites could not be assigned to a 95% confidence risk category. Uninfected *I. scapularis* populations were also identified along two of these putative expansion fronts (Illinois/Indiana and New York/Vermont), consistent with a pattern of initial tick spread followed by the spread of *B. burgdorferi*.[34] An alternative invasion pattern was detected in Michigan,[33] where low-prevalence *B. burgdorferi* infection was detected in other tick species and in wildlife at inland sites before the arrival of *I. scapularis*. The authors suggested a cryptic *B. burgdorferi* transmission cycle by other vector-competent tick species in the absence of *I. scapularis*. Further studies are warranted to evaluate the accuracy of the predictive model and to describe the patterns and processes driving the expansion of *I. scapularis* and *B. burgdorferi*.

The model performed poorly in western Pennsylvania, underestimating the density of infected nymphs at Parker Dam State Park in northern Clearfield County and in Presque Isle State Park in Erie County. *Borrelia burgdorferi* was previously detected in *Peromyscus leucopus* in Elk County, north of Clearfield County,[35] and both *I. scapularis* and *B. burgdorferi* were previously reported in Erie County.[36] Low estimated density of infected nymphs at these sites is caused by their isolation from other high-density sites, resulting in low values of the autocovariate term. In addition, Parker Dam State Park's high elevation (490 m), near the limit of the nymphal distribution identified by our study (510 m), further reduced the density estimate for this site. The isolation of these infected tick populations suggests a separate Lyme disease focus from the known northeastern and midwestern foci[37]; further study is needed to determine the extent of these isolated Pennsylvania foci.

The spatial pattern of infected nymphs was highly consistent with the distribution of all nymphs found in our previous model,[14] suggesting that nymphal density, rather than infection prevalence, drives the spatial patterns in acarological risk. No obvious spatial structure was detected in the distribution of nymphal infection prevalence (Figure 4). However, low precision of the infection prevalence estimates because of small sample sizes at the site level limit any inferences beyond a regional level.

The probability of finding nymphs was driven by elevation, VPDm, and seasonal variation in temperature. These variables were selected for use in the current model because of their predictive value for the density of *I. scapularis* nymphs.[12] The density of host-seeking ticks of Lyme disease vectors in Europe has been found to decrease with increasing elevation[38,39]; the extent to which this effect is caused by temperature remains to be determined. The strong predictive power of VPD on the density of host-seeking nymphs is consistent with other studies.[40–42] Water stress and high temperatures are hypothesized to regulate tick populations by decreasing tick survival during off-host periods[43] and regulating host-seeking activity.[44–47]

Seasonality in temperature has also been an important predictor in other studies of the distribution of vectors and disease,[48] including tick-borne diseases.[49] Temporal Fourier analysis captures both the extremes in temperature and the rates of fall cooling and spring warming. Extreme winter temperatures can limit the northern distribution of ticks by directly killing the ticks,[43,50] inhibiting host-seeking activity,[44,46,47] or limiting the availability of hosts.[51] The high rate of fall cooling can also affect tick population dynamics by limiting the time available for larvae to find a host in the fall, thus entering diapause unfed,[52] which potentially increases their mortality rate.[52] On the other hand, high rates of spring warming may have an opposite effect, because it would result in faster accumulation of degree-days for development, potentially leading to earlier egg deposition and larval emergence.[51]

Previous studies identified a positive link between forest fragmentation and both tick density and infection prevalence.[19,20] Extensive data mining of our dataset did not identify any significant landscape predictors of nymphal infection prevalence (results not shown), and the only landscape predictor included in the final regression model reflected a negative, rather than positive, link between forest fragmentation and the density of infected nymphs. The larger spatial extent and coarser spatial scale of this study may partially explain differences with previous studies.[53] Forest fragmentation metrics were calculated for each 8 km × 8 km pixels in this work, although previous studies focused on a scale of a few hectares[19] to 0.5 km.[20] At the resolution of our study, highly urbanized or agricultural areas appear as highly fragmented pixels, whereas lower fragmentation is linked to more forested areas that typically support *I. scapularis* populations. A limitation of this study is that sampling was limited to natural areas to standardize sampling at a continental scale. However, human risk for Lyme disease appears to be peridomestic, at least in the northeastern United States.[54,55] More studies on the associations between the density of infected nymphs and human risk at different scales are warranted.

In terms of public health applications, the lack of spatial structure in nymphal infection prevalence, combined with the difficulty in accurately estimating prevalence with small sample sizes, brings into question the validity of using an exact prevalence threshold to guide clinical decisions on treatment, such as the current recommendation of tick-bite prophylaxis when infection prevalence is > 0.2.[9] Our results indicate that the presence of any number of infected nymphs may be considered sufficient to recommend post-exposure prophylaxis. Infected nymphs were found in 92.3% of the sites where a threshold of 14 nymphs per 1,000 m^2 were collected.

The construction of an accurate map showing the spatial distribution and density of *I. scapularis* in the United States has been limited by the use of non-standardized, county-based data on the distribution of *I. scapularis*,[15] the mapping of all *I. scapularis* life stages,[56,57] and the absence of data on nymphal infection with *B. burgdorferi*.[14] The Lyme disease risk map that we present here is based on standardized sampling of infected host-seeking *I. scapularis* nymphs, the primary vector stage of *B. burgdorferi* for humans throughout the geographic range of the species. Although the large spatial extent of this map necessarily limits its spatial resolution and localized studies are warranted in some focal areas, our map makes new contributions to surveillance, prevention, and control programs. Specifically, this risk map can assist in surveillance and control programs by identifying regions where human cases are expected and may assist treatment decisions such as the use of antimicrobial prophylaxis following a tick bite. Finally, this map provides an essential baseline for tracking spread of the infection from areas endemic in 2004–2007.

Received June 21, 2011. Accepted for publication October 9, 2011.

Note: Supplemental appendix, table and figure appear at www.ajtmh.org.

Acknowledgments: We thank the 80 field assistants who made this project possible. Special thanks to Tim Andreadis, Katherine Watkins, Laura Kramer, Jessica Payne, Elizabeth Racz, Kelly Liebman, Liza Lutzker, and David Boozer for tick identification and logistic support; Carlos Diuk for database support; Brad Lobitz and Andrew Michaelis for technical assistance; Dennis Grove, Lindsay Rollend, and Russell Barbour for arranging collection permits. We also acknowledge Corrine Folsom-O'Keefe for manuscript editing and Kimberly Tsao for helpful comments, and John Brownstein and Ben Beard for their early contributions to this work.

Financial support: This project was funded by CDC-Division of Vector-Borne Infectious Diseases Cooperative Agreement No. CI00171-01.

Authors' addresses: Maria A. Diuk-Wasser and Paul Cislo, Division of Epidemiology of Microbial Diseases, Yale School of Public Health, New Haven, CT, E-mails: maria.diuk@yale.edu and prcislo@juno.com. Anne Gatewood Hoen, Community and Family Medicine, Dartmouth Medical School, Lebanon, NH, E-mail: Anne.G.Hoen@dartmouth.edu. Robert Brinkerhoff, Biology Department, University of Richmond, Richmond, VA, E-mail: jbrinker@richmond.edu. Sarah A. Hamer and Jean I. Tsao, Department of Fisheries and Wildlife, Michigan State University, East Lansing, MI, E-mails: hamer@msu.edu and tsao@msu.edu. Michelle Rowland, Magee-Women's Hospital of UPMC, Pittsburgh, PA, E-mail: rowlandmr@upmc.edu. Roberto Cortinas, Department of Entomology, University of Nebraska, Lincoln, NE, E-mail: rcortinas@unlnotes.unl.edu. Gwenaël Vourc'h, Institut National de la Recherche Agronomique, Saint Genès Champanelle, France, E-mail: gvourch@clermont.inra.fr. Forrest Melton, California State University, Monterey Bay, Seaside, CA, E-mail: Forrest.S.Melton@nasa.gov. Graham Hickling, Department of Forestry, Wildlife and Fisheries, University of Tennessee, Knoxville, TN, E-mail: ghicklin@utk.edu. Jonas Bunikis, Vilnius University, Vilnius, Lithuania, E-mail: Jonas.BUNIKIS@ec.europa.e. Alan G. Barbour, Department of Microbiology and Molecular Genetics, University of California, Irvine, CA, E-mail: abarbour@uci.edu. Uriel Kitron, Department of Environmental Studies, Emory University, Atlanta, GA, E-mail: ukitron@emory.edu. Joseph Piesman, Division of Vector-Borne Infectious Diseases, Centers for Disease Control and Prevention, Fort Collins, CO, E-mail: jfp2@CDC.GOV.

REFERENCES

1. Steere AC, Hardin JA, Malawista SE, 1977. Lyme arthritis: the enlarging clinical spectrum. *Clin Res 25:* 368A.
2. Steere AC, 1989. Lyme disease. *N Engl J Med 321:* 586–596.
3. Steere AC, Hardin JA, Malawista SE, 1977. Erythema chronicum migrans and Lyme arthritis: cryoimmunoglobulins and clinical activity of skin and joints. *Science 196:* 1121–1122.
4. Bacon RM, Kugeler KJ, Mead PS, 2008. Surveillance for Lyme disease—United States, 1992–2006. *MMWR Surveill Summ 57:* 1–9.
5. Shadick NA, Phillips CB, Logigian EL, Steere AC, Kaplan RF, Berardi VP, Duray PH, Larson MG, Wright EA, Ginsburg KS, Katz JN, Liang MH, 1994. The long-term clinical outcomes of Lyme disease. A population-based retrospective cohort study. *Ann Intern Med 121:* 560–567.
6. Nadelman RB, Arlin Z, Wormser GP, 1991. Life-threatening complications of empiric ceftriaxone therapy for seronegative Lyme disease. *South Med J 84:* 1263–1264.
7. Holzbauer SM, Kemperman MM, Lynfield R, 2010. Death due to community-associated *Clostridium difficile* in a woman receiving prolonged antibiotic therapy for suspected Lyme disease. *Clin Infect Dis 51:* 369–370.
8. Aguero-Rosenfeld ME, Wang GQ, Schwartz I, Wormser GP, 2005. Diagnosis of Lyme borreliosis. *Clin Microbiol Rev 18:* 484–501.
9. Wormser GP, Dattwyler RJ, Shapiro ED, Halperin JJ, Steere AC, Klempner MS, Krause PJ, Bakken JS, Strie F, Stanek G, Bockenstedt L, Fish D, Dumler JS, Nadelman RB, 2006. The clinical assessment, treatment, and prevention of Lyme disease, human granulocytic anaplasmosis, and babesiosis: clinical practice guidelines by the infectious diseases society of America. *Clin Infect Dis 43:* 1089–1134.
10. Center for Disease Control and Prevention, 2010. Reported cases of Lyme disease–United States, 2009. Available at: http://www.cdc.gov/ncidod/dvbid/lyme/ld_incidence.htm. Accessed October 21, 2010.
11. Mather TN, Nicholson MC, Donnelly EF, Matyas BT, 1996. Entomologic index for human risk of Lyme disease. *Am J Epidemiol 144:* 1066–1069.
12. Reisen WK, 2010. Landscape epidemiology of vector-borne diseases. *Annu Rev Entomol 55:* 461–483.
13. Falco RC, McKenna DF, Daniels TJ, Nadelman RB, Nowakowski J, Fish D, Wormser GP, 1999. Temporal relation between *Ixodes scapularis* abundance and risk for Lyme disease associated with erythema migrans. *Am J Epidemiol 149:* 771–776.
14. Diuk-Wasser M, Vourc'h G, Cislo P, Gatewood Hoen A, Melton F, Hamer S, Rowland M, Hickling GS, Tsao JI, Barbour AG, Kitron U, Piesman J, Fish D, 2010. Field and climate-based model for predicting the density of host-seeking nymphal *Ixodes scapularis*, an important vector of tick-borne disease agents in the eastern United States. *Glob Ecol Biogeogr 19:* 504–514.
15. Dennis DT, Nekomoto TS, Victor JC, Paul WS, Piesman J, 1998. Reported distribution of *Ixodes scapularis* and in *Ixodes pacificus* (Acari: Ixodidae) in the United States. *J Med Entomol 35:* 629–638.
16. Falco RC, Fish D, 1992. A comparison of methods for sampling the deer tick, *Ixodes dammini*, in a Lyme disease-endemic area. *Exp Appl Acarol 14:* 165–173.
17. Fish D, 1993. Population ecology of *Ixodes dammini*. Ginsberg HS, ed. *Ecology and Environmental Management of Lyme Disease*. New Brunswick, NJ: Rutgers University Press, 25–42.
18. Tsao JI, Wootton JT, Bunikis J, Luna MG, Fish D, Barbour AG, 2004. An ecological approach to preventing human infection: vaccinating wild mouse reservoirs intervenes in the Lyme disease cycle. *P Natl Acad Sci USA 101:* 18159–18164.
19. Allan BF, Keesing F, Ostfeld RS, 2003. Effect of forest fragmentation on Lyme disease risk. *Conserv Biol 17:* 267–272.
20. Brownstein JS, Skelly DK, Holford TR, Fish D, 2005. Forest fragmentation predicts local scale heterogeneity of Lyme disease risk. *Oecologia 146:* 469–475.
21. Homer C, Huang CQ, Yang LM, Wylie B, Coan M, 2004. Development of a 2001 national land-cover database for the United States. *Photogramm Eng Remote Sensing 70:* 829–840.
22. Agarwal DK, Gelfand AE, Citron-Pousty S, 2002. Zero-inflated models with application to spatial count data. *Environ Ecol Stat 9:* 341–355.
23. Spielman A, Wilson ML, Levine JF, Piesman J, 1985. Ecology of *Ixodes dammini*-borne human babesiosis and Lyme disease. *Annu Rev Entomol 30:* 439–460.

24. Pinger RR, Timmons L, Karris K, 1996. Spread of *Ixodes scapularis* (Acari: Ixodidae) in Indiana: collections of adults in 1991–1994 and description of a *Borrelia burgdorferi*-infected population. *J Med Entomol 33:* 852–855.
25. Barbour AG, Fish D, 1993. The biological and social phenomenon of Lyme disease. *Science 260:* 1610–1616.
26. Dormann CF, McPherson JM, Araujo MB, Bivand R, Bolliger J, Carl G, Davis R, Hirzel A, Jetz W, Kissling WD, Kühn I, Ohlemüller R, Peres-Neto PR, Reineking B, Schröder B, Schurr FM, Wilson R, 2007. Methods to account for spatial autocorrelation in the analysis of species distributional data: a review. *Ecography 30:* 609–628.
27. Goddard J, Piesman J, 2006. New records of immature *Ixodes scapularis* from Mississippi. *J Vector Ecol 31:* 421–422.
28. Cilek JE, Olson MA, 2000. Seasonal distribution and abundance of ticks (Acari: Ixodidae) in northwestern Florida. *J Med Entomol 37:* 439–444.
29. Falco RC, Fish D, 1988. A survey of tick bites acquired in a Lyme disease-endemic area in southern New York State. *Ann N Y Acad Sci 539:* 456–457.
30. Rand PW, Lacombe EH, Dearborn R, Cahill B, Elias S, Lubelczyk CB, Beckett GA, Smith RPJr, 2007. Passive surveillance in Maine, an area emergent for tick-borne diseases. *J Med Entomol 44:* 1118–1129.
31. Pinger RR, Holycross J, Ryder J, Mummert M, 1991. Collections of adult *Ixodes dammini* in Indiana, 1987–1990, and the isolation of *Borrelia burgdorferi*. *J Med Entomol 28:* 745–749.
32. White DJ, Chang HG, Benach JL, Bosler EM, Meldrum SC, Means RG, Debbie JG, Birkhead GS, Morse DL, 1991. The geographic spread and temporal increase of the Lyme disease epidemic. *JAMA 266:* 1230–1236.
33. Hamer SA, Tsao JI, Walker ED, Hickling GJ, 2010. Invasion of the Lyme disease vector *Ixodes scapularis*: implications for *Borrelia burgdorferi* endemicity. *EcoHealth 7:* 47–63.
34. Madhav NK, Brownstein JS, Tsao JI, Fish D, 2004. A dispersal model for the range expansion of blacklegged tick (Acari: Ixodidae). *J Med Entomol 41:* 842–852.
35. Lord RD, Lord VR, Humphreys JG, Mclean RG, 1994. Distribution of *Borrelia burgdorferi* in host mice in Pennsylvania. *J Clin Microbiol 32:* 2501–2504.
36. Courtney JW, Dryden RL, Wyleto P, Schneider BS, Massung RF, 2003. Characterization of *Anaplasma phagocytophila* and *Borrelia burgdorferi* genotypes in *Ixodes scapularis* ticks from Pennsylvania. *Ann N Y Acad Sci 990:* 131–133.
37. Spielman A, Levine JF, Wilson ML, 1984. Vectorial capacity of North American *Ixodes* ticks. *Yale J Biol Med 57:* 507–513.
38. Jouda F, Perret JL, Gern L, 2004. *Ixodes ricinus* density and distribution and prevalence of *Borrelia burgdorferi* sensu lato infection along an altitudinal gradient. *J Med Entomol 41:* 162–169.
39. Cadenas FM, Rais O, Jouda F, Douet V, Humair PF, Moret J, Gern L, 2007. Phenology of *Ixodes ricinus* and infection with *Borrelia burgdorferi* sensu lato along a north- and south-facing altitudinal gradient on Chaumont Mountain, Switzerland. *J Med Entomol 44:* 683–693.
40. Estrada-Pena A, 2002. Increasing habitat suitability in the United States for the tick that transmits Lyme disease: a remote sensing approach. *Environ Health Perspect 110:* 635–640.
41. Guerra M, Walker E, Jones C, Paskewitz S, Cortinas MR, Stancil A, Beck L, Bobo M, Kitron U, 2002. Predicting the risk of Lyme disease: habitat suitability for *Ixodes scapularis* in the north central United States. *Emerg Infect Dis 8:* 289–297.
42. Brownstein JS, Holford TR, Fish D, 2003. A climate-based model predicts the spatial distribution of the Lyme disease vector *Ixodes scapularis* in the United States. *Environ Health Perspect 111:* 1152–1157.
43. Ogden NH, Lindsay LR, Beauchamp G, Charron D, Maarouf A, O'Callaghan CJ, Waltmer-Toews D, Barker IK, 2004. Investigation of relationships between temperature and developmental rates of tick *Ixodes scapularis* (Acari: Ixodidae) in the laboratory and field. *J Med Entomol 41:* 622–633.
44. Vail SG, Smith G, 1998. Air temperature and relative humidity effects on behavioral activity of blacklegged tick (Acari: Ixodidae) nymphs in New Jersey. *J Med Entomol 35:* 1025–1028.
45. Randolph SE, Storey K, 1999. Impact of microclimate on immature tick-rodent host interactions (Acari: Ixodidae): implications for parasite transmission. *J Med Entomol 36:* 741–748.
46. Perret JL, Guigoz E, Rais O, Gern L, 2000. Influence of saturation deficit and temperature on *Ixodes ricinus* tick questing activity in a Lyme borreliosis-endemic area (Switzerland). *Parasitol Res 86:* 554–557.
47. Schulze TL, Jordan RA, 2003. Meteorologically mediated diurnal questing of *Ixodes scapularis* and *Amblyomma americanum* (Acari: Ixodidae) nymphs. *J Med Entomol 40:* 395–402.
48. Scharlemann JP, Benz D, Hay SI, Purse BV, Tatem AJ, Wint GR, Rogers DJ, 2008. Global data for ecology and epidemiology: a novel algorithm for temporal Fourier processing MODIS data. *PLoS ONE 3:* e1408.
49. Randolph SE, 2000. Ticks and tick-borne disease systems in space and from space. *Adv Parasitol 47:* 217–243.
50. Rand PW, Holman MS, Lubelczyk C, Lacombe EH, DeGaetano AT, Smith RP, 2004. Thermal accumulation and the early development of *Ixodes scapularis*. *J Vector Ecol 29:* 164–176.
51. Lindsay LR, Barker IK, Surgeoner GA, Mcewen SA, Gillespie TJ, Robinson JT, 1995. Survival and development of *Ixodes-Scapularis* (Acari, Ixodidae) under various climatic conditions in Ontario, Canada. *J Med Entomol 32:* 143–152.
52. Yuval B, Spielman A, 1990. Duration and regulation of the developmental cycle of *Ixodes-Dammini* (Acari, Ixodidae). *J Med Entomol 27:* 196–201.
53. Killilea ME, Swei A, Lane RS, Briggs CJ, Ostfeld RS, 2008. Spatial dynamics of Lyme disease: a review. *EcoHealth 5:* 167–195.
54. Dister SW, Fish D, Bros SM, Frank DH, Wood BL, 1997. Landscape characterization of peridomestic risk for Lyme disease using satellite imagery. *Am J Trop Med Hyg 57:* 687–692.
55. Frank DH, Fish D, Moy FH, 1998. Landscape features associated with Lyme disease risk in a suburban residential environment. *Landscape Ecol 13:* 27–36.
56. Centers for Disease Control and Prevention, 1999. Morbidity and Mortality Weekly Report. Available at: http://www.cdc.gov/mmwr/preview/mmwrhtml/rr4807a2.htm. Accessed May 1, 2005.
57. Brownstein JS, Holford TR, Fish D, 2003. A climate-based model predicts the spatial distribution of the Lyme disease vector *Ixodes scapularis* in the United States. *Environ Health Perspect 111:* 1152–1157.